

A NEW APPROACH FOR MITIGATING BIOFOULING BY PROMOTING ONLINE CLEANING USING A SACRIFICIAL PARAFFIN COATING

Q. Yang¹, D.I. Wilson², S. Chang¹ and L. Shi¹

¹ Key Laboratory for Thermal Science and Power Engineering of Ministry of Education, Department of Thermal Engineering, Tsinghua University, Beijing 100084, PR China. E-mail (L.Shi): rxsl@mail.tsinghua.edu.cn

² Department of Chemical Engineering and Biotechnology, New Museums Site, Pembroke Street, Cambridge, CB2 3RA, UK

ABSTRACT

The presence of biofouling layers on heat transfer surfaces can reduce heat transfer efficiency markedly. This paper reports a new paraffin coating method for inhibiting biofouling growth and promoting rapid online cleaning in exchangers recovering thermal energy from treated aqueous sewage streams. The paraffin wax coating is cast in place without needing to disassemble the device, while the low roughness and hydrophobicity of the coating inhibit bacterial growth. The coating and any attached biofouling can be removed by raising the surface temperature above the wax melting point. The effectiveness of this online cleaning and inhibition strategy was investigated using a simple laboratory test channel, representing a plate heat exchanger, and a model fluid simulating treated sewage. The thermal resistance and deposit morphology were monitored. The reduction in biofouling thermal resistance outweighs the additional thermal resistance resulting from the coating. A short techno-economic analysis is presented to further discuss the advantage of paraffin coating.

INTRODUCTION

Treated sewage contains large amounts of low grade energy, which has prompted the recent rapid development of treated sewage source heat pump systems (TSSHPS) (Tian *et al.*, 2012a). However, the high bacterial concentration and rich nutrient environment of treated sewage results in significant levels of biofouling (Tian *et al.*, 2012b), which markedly impairs the heat transfer efficiency and coefficient of performance (COP) of TSSHPS (Shi *et al.*, 2009).

The use of surface coatings for inhibiting biofouling is a promising approach which has attracted much attention recently (Sokolova *et al.*, 2012; Olsen *et al.*, 2009; Vladkova, 2008). The role of the coating can be to inhibit biofouling in general (Scardino and Nys, 2010), reduce bacterial activity (Elangovan *et al.*, 2012), change contact angle (Sen *et al.*, 2012; Wang *et al.*, 2011) or modify other physical properties of the surface affecting biofouling attachment and detachment (Hwang *et al.*, 2012; Bonin *et al.*, 2012; Raulio *et al.*, 2008). Reducing the extent and rate of fouling extends the length of time between cleaning operations.

A second mitigation strategy is to improve the effectiveness and rate of on-line cleaning. Significant time and cost savings can be achieved by avoiding manual cleaning, which usually requires disassembly of the heat exchanger (Jalalirad *et al.*, 2012; Georgiadis and Papageorgiou, 2000). However, most on-line biofouling cleaning methods are not sufficiently thorough and regular disassembly and manual cleaning are still necessary (Müller-Steinhagen *et al.*, 2005).

This paper reports a new approach that combines surface coating and online cleaning. A sacrificial coating has been developed which can be applied *in situ*, inhibits the growth of biofouling layers under normal process conditions, and can be readily removed by manipulating the temperature during a cleaning operation. Any biofouling layer is removed along with the coating during the cleaning cycle, eliminating the need to disassemble the exchanger. The coating material is a paraffin wax, which combines effectiveness in inhibiting biofouling due to its low roughness and hydrophobicity (Christine *et al.*, 2000; Carl *et al.*, 2012) with the melting and solidification properties that allow coating and removal using readily achievable temperatures.

The concept of sacrificial coating has been advocated and/or implemented in various forms and application areas, such as the manufacture of microfiltration membranes (Li *et al.*, 2008) and corrosion protection for metal surfaces (Schmidt *et al.*, 2006). Sacrificial coatings are usually pre-coated by an external process and eliminated by triggers such as pH or salt concentration (De Vos *et al.*, 2010). The paraffin sacrificial coating method described here uses the same approach, of adding a thin layer to protect a surface (Wilson and Harvey, 1989): the trigger in this case is temperature. The novel differences lie in the paraffin coating offering both fouling inhibition and enhanced cleaning, as well as being cast and removed in place in repeated cycles, which is required for TSSHPS heat exchanger service.

This paper reports an experimental investigation of the in-situ paraffin coating concept. Experiments were performed to test the feasibility of the in-situ coating method using a simple rectangular duct heat exchanger representing the flow channels in a plate heat exchanger. The coating layer thickness, contact angle, surface roughness and additional thermal resistance generated by the coating, R_{add} ,

were measured. The performance of the coating under fouling conditions was monitored, as well as the residual thermal resistance, R_{res} , following several fouling and cleaning cycles. A techno-economic analysis of the approach is presented which considers the attractiveness of the technology for TSSHPS applications and areas for future development are suggested.

MATERIALS AND METHODS

Paraffin coating system and heat exchange test section

The paraffin used for coatings was a fully refined wax with a melting point in the range of 60~62 °C. Between 53-60 °C the paraffin exists as a soft solid which trial tests showed could be easily flushed away by the liquid flow. Plate interface temperatures below 53 °C are therefore required for the paraffin coating process. This can be achieved by specifying appropriate temperature distributions. Treated sewage temperature in TSSHPS applications rarely exceeds 40 °C, under which conditions the paraffin coating exists as a rigid solid layer when in use.

The heat transfer system used for coating and biofouling studies is shown in Figure 1. The coating stage did not require the use of the feed tanks, peristaltic pump and overflow drainage (*i.e.* biofouling section). The coating mixture was prepared by adding molten paraffin at 70 °C to deionised water, also at 70 °C, in a thermostatted bath with vigorous stirring for 5 minutes to generate a turbid emulsion. The emulsion was circulated through the heat exchange channel by a centrifugal pump (Julabo ED F12, 4L, Germany).

A separate centrifugal pump circulated the heat transfer medium, deionised water, from another thermostatted water bath through the heat exchange test section. All connections were 10 mm silicone tubing (sterilized at 121 °C for 30 min).

Figure 2 shows a detailed schematic of the heat exchange test section. The two flow channels were identical, with internal dimensions: 200 mm (long) ×35 mm (wide) ×2 mm (height). A 1 mm thick 316 stainless steel (SS) plate separated the two flow channels and serves as the heat transfer surface. The plate surface roughness, R_a , was measured as 500 ± 50 nm using a surface mapping microscope (Micro XAM, ADE Inc., USA).

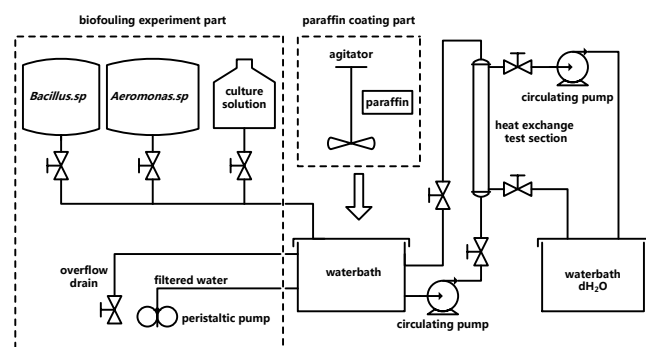


Fig. 1 Schematic of experimental system. Dashed lines delineate the paraffin coating and biofouling sections. dH₂O – deionised water.

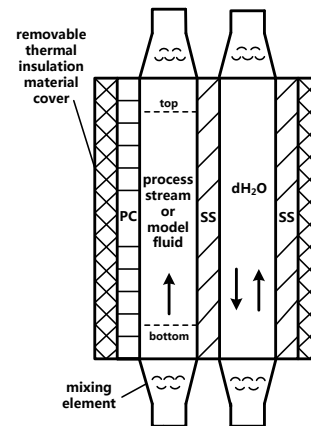


Fig. 2 Schematic of heat exchange test section. The heat transfer medium (deionised water, dH₂O) be either upward (co-current) or downward (counter current). PC – polycarbonate; SS – 316 stainless steel.

Paraffin coatings were formed on the process stream side of the heat transfer surface. No fouling deposition was observed on the heat transfer medium side. The outer walls of the test section were constructed from polycarbonate to allow online observation and measurement. Counter-current and co-current configurations were implemented by connecting the heat transfer medium inlet to the corresponding end of the test section. The co-current configuration was employed for paraffin coating as this configuration gives a more uniform temperature profile along the channel, and therefore more uniform layer thickness (discussed below, Figure 3(a)).

Coating

In order to make a thin yet complete coating, the temperature distribution and paraffin concentration need to be selected carefully. A high concentration can give a thick layer with poor thermal performance, whereas a low concentration may give incomplete coverage. The tests reported here used a paraffin concentration of 20 g L⁻¹. The optimum concentration may vary according to device configuration, materials, settings and processes.

The paraffin-water emulsion (process stream) was circulated through the test section at 70 °C with the heat transfer medium temperature initially at 70 °C. The latter temperature was then reduced to 20 °C and the emulsion circulated for a further 5 min. The flow velocities of both sides were 0.2 m s⁻¹. The system was then drained.

Figure 3(a) shows the temperature profile along the test section at the start of coating experiments, calculated using the Fluent 6.3 computational fluid dynamics software package. The temperature of the process stream - plate interface varies from 49 to 53 °C, *i.e.* around 10 K below the melting point of paraffin, and is expected to give a relatively rigid layer.

Coatings formed at higher surface temperatures were fluffy and were readily ruptured and flushed away by the process stream in heat transfer operation: 53 °C represents the operational limit for a rigid paraffin coating for layers to

withstand the shear stress imposed by the process stream in these studies.

The estimated initial temperature distributions across the heat transfer elements at the (a) inlet and (b) outlet, extracted from the simulations, are plotted in Figure 4. The large temperature gradient across the thermal boundary layer also helps the formation of paraffin deposit as it gives a high cooling rate at the surface. It also helps to control the layer thickness, giving a thin and rigid paraffin layer.

The coating process is self-limiting as it is performed with a constant overall temperature driving force. Figure 3(b) shows the temperature distribution anticipated for a wax deposit layer of uniform thickness of 10 μm, giving an additional thermal resistance, R_{add} , of $0.5 \times 10^{-4} \text{ m}^2\text{K W}^{-1}$. Experimental data reported below show this to be a representative coating thickness: the R_{add} value is based on a thermal conduction resistance, given by thickness/thermal conductivity, of $\sim 0.4 \times 10^{-4} \text{ m}^2\text{K W}^{-1}$, and a thermal contact resistance of $0.1 \times 10^{-4} \text{ m}^2\text{K W}^{-1}$. Figure 3(b) shows that the emulsion–deposit layer interface temperature varies from 50 to 56 °C. These values are on average 2 K higher than the clean values. The increase in interface temperature will reduce the rigidity of the newly formed deposit and ultimately result in newly formed material being flushed off. The deposit thickness is therefore controlled by wax concentration, coating time, flow velocity, contacting arrangement and temperature distribution.

Paraffin coating properties

The paraffin layer was examined and its thickness measured *in situ* by an Olympus STM6 measuring microscope with a calibrated z-axis function. Figure 5 shows the stainless steel surface (a) before and (b) after coating. More than 95% of the surface was covered, with the layer thickness ranging from 5-10 μm. The thickness was measured at 9 randomly chosen locations. The mean thickness was $6.3 \pm 2 \text{ μm}$ for the first coating cycle on the stainless steel surface. The thermal conductivity of the pure paraffin was measured separately as $0.27 \text{ W m}^{-1}\text{K}^{-1}$ at 25 °C (Hotdisk TPS 2500, Sweden).

The contact angle of the uncoated and coated surfaces was measured using a Nikon CCD camera and images such as those in Figure 6(i) processed using the ImageJ (NIH, USA) software package. The contact angle for deionised water changed from around 68 ° to 122 °, indicating a change from hydrophilic to hydrophobic interaction. The surface topology also changed, as shown in Figure 6(ii), with R_a values decreasing from $500 \pm 50 \text{ nm}$ to $160 \pm 50 \text{ nm}$ (Micro XAM, ADE Inc., USA). Both the hydrophobicity and reduction in surface roughness are expected to contribute to biofouling inhibition.

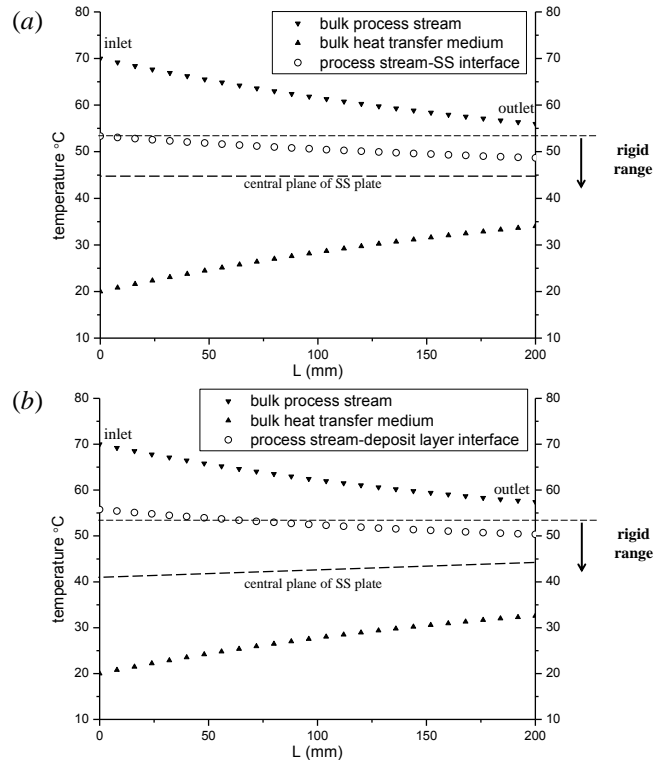


Fig. 3 Temperature distribution along the test section in coating mode. (a) Initial, clean surface; (b) surface with uniform 10 μm thick wax coating. Horizontal dashed line indicates the temperature at the midpoint of the SS plate (45 °C at clean condition).

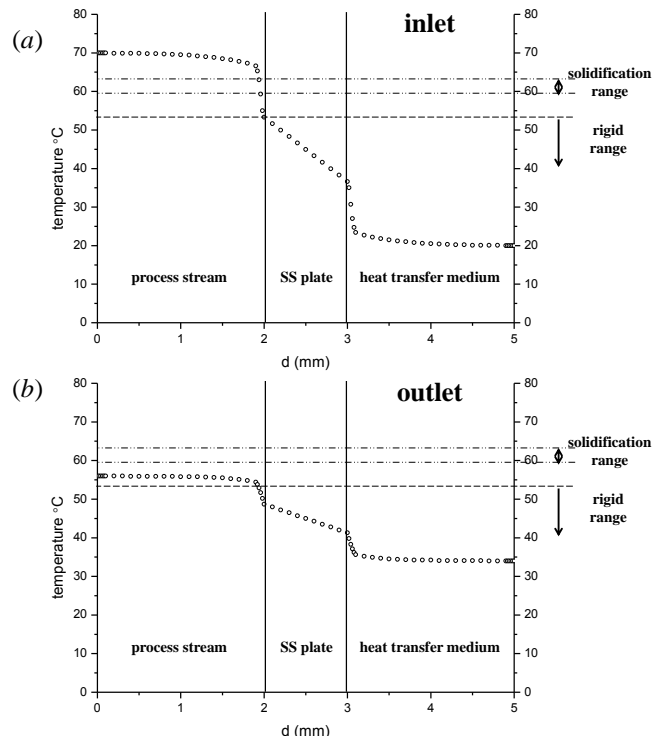


Fig. 4 Estimated temperature distribution across the test plate under clean conditions (see Figure 3(a)) at the test section (a) inlet and (b) outlet. Salient temperatures for wax formation marked by dashed horizontal lines.

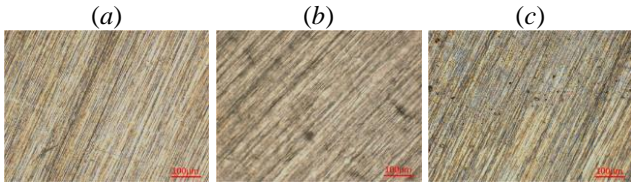


Fig. 5 Photographs of (a) uncoated SS surface; (b) paraffin coated surface; (c) residual material after online cleaning. Scale bar is 100 μm long.

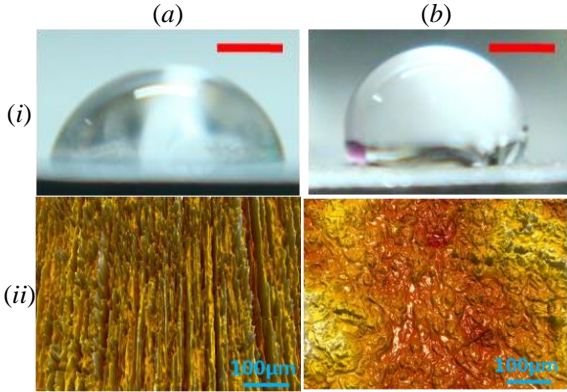


Fig.6 (i) Photographs of 2 μL water droplets showing effect of coating on contact angle (scale bar = 1 mm). (ii) Micrographs comparing roughness (scale bar = 100 μm). (a) SS surface and (b) paraffin coated surface.

Biofouling tests

Biofouling tests employed the counter-current configuration as this reflects the operating mode in industrial treated sewage heat recovery systems and offer a more robust configuration for fouling service (Yang *et al.*, 2013).

The water quality and bacterial population of treated sewage in six Beijing sewage plants was monitored for over a year to establish the composition and operating parameters for a laboratory model fluid. The model fluid formulation in Table 1 was selected to match the water quality parameters including BOD, pH, temperature and concentration of inorganic ions in the treated sewage.

Polymerase chain reaction (PCR) and 16srRNA analysis of the treated sewage bacterial populations indicated that *Bacillus.sp* (Gram positive) and *Aeromonas.sp* (Gram negative) accounted for over 80% of the biomass in suspension and 95% of the organisms forming biofilms. In biofilms generated in the absence of paraffin coatings, *Bacillus.sp* was found to predominate in terms of cell quantity while *Aeromonas.sp* contributed more to secretion of extracellular polymeric substances. Detailed analysis of biofilms formed on the paraffin coated surfaces was not performed in these tests. The laboratory model fluid was also formulated to match the bacterial concentration and population. Stocks of *Bacillus.sp* and *Aeromonas.sp* were cultivated separately in sterile broth medium in an orbital shaker (30 °C, 200 rpm) for 24 h after inoculation. The total concentration of bacteria in the model fluid was diluted to $5 \pm 0.2 \times 10^4$ CFU ml⁻¹ and the ratio of *Bacillus sp.* to *Aeromonas sp.* was 1:1.

Table 1. Model fluid composition and operating conditions

Parameter	Value	Control method
Bacteria concentration	$5 \pm 0.2 \times 10^4$ CFU ml ⁻¹	Diluted cultivated bacteria solutions
<i>Bacillus.sp</i> : <i>Aeromonas.sp</i>	1:1	Solutions fed in equal amounts
Temperature	25 °C	Thermostatted bath
BOD	15 mg L ⁻¹	Glucose solution
pH	7.2	Diluted NaOH solution
Ca ²⁺	65 mg L ⁻¹	Stable natural background
Mg ²⁺	25 mg L ⁻¹	Stable natural background
Dissolved oxygen	6.6~7.1 mg L ⁻¹	Stable natural background

The biofouling apparatus is shown in Figure 1. The model fluid was held in a thermostatted water bath and was circulated through the heat exchange flow channel as before. The composition of the model fluid was maintained by gravity feed of micro-organism suspensions and culture solution, a peristaltic pump feeding filtered water, and an overflow to maintain the liquid volume constant at $4 \text{ L} \pm 1\%$. The model solution was replaced at 30 minute intervals. Deionised (non-fouling) water was used as the heat transfer medium and was circulated at the same flow rate as the model fluid, with a flow velocity on both sides of 0.2 m s^{-1} . Reynolds number and wall shear stress were 800 and 0.7Pa for 25 °C condition.

The temperature of both inlet and outlet streams were measured every two minutes using K type thermocouples connected to a data logging PC (Agilent 34972A, USA). The uncertainty in these measurements was ± 0.2 K. The thermal resistance of the test section, *R*, was calculated from the change in overall heat transfer coefficient, *U*, via

$$R = \frac{1}{U} - \frac{1}{U_0} \tag{1}$$

where *U*₀ is the initial value for a clean, uncoated, surface. The uncertainty in *R* was $\pm 5\%$. The additional thermal resistance introduced by paraffin layer before fouling is labelled *R*_{add}. The residual thermal resistance following an online cleaning stage was calculated using clean solutions and was labeled *R*_{res}.

The additional thermal resistance *R*_{add} resulting from the presence of the paraffin layer was modeled as arising from two contributions:

$$R_{\text{add}} = R_{\text{add,P}} + R_{\text{add,C}} \tag{2}$$

Here *R*_{add,P} is the resistance due to conduction through the paraffin layer, estimated as paraffin layer thickness divided

by its thermal conductivity. $R_{add,C}$ is a thermal contact resistance, estimated by difference, which quantifies the impairment of heat transfer due to gaps in the paraffin–SS interface.

The thermal resistance due to the biofilm, R_f was estimated from

$$R_f = R - R_{add} \quad (3)$$

R_{add} was assumed to be constant over a given fouling cycle.

Fouling experiments were run for 5 days, during which time a fouling layer formed on top of the paraffin layer. This was then removed by online cleaning and the paraffin coating re-applied. The cleaning and coating cycle lasted 0.5 day altogether. Heat transfer operations were then restarted. Five cycles of paraffin coating and online cleaning were conducted, lasting 27.5 days in total. Biofouling experiments employed counter-current flow, with heat transfer medium and model fluid inlet temperatures of 35 °C and 25 °C, as reported in Yang *et al.* (2013). The mean flow velocity was 0.2 m s⁻¹ on both sides.

Online cleaning operation

Deionised water at 70 °C was circulated through both sides of the test cell in the co-current configuration at a mean velocity of 1 m s⁻¹ for 20 min. This melted the paraffin layer and flushed it away from the surface. Since most of biofilm grew on top of the paraffin layer, the majority of the biofouling layer was removed by this step, as shown in Figure 5(c). Sporadic patches of residual paraffin layer or biofilm were visible on the surface after the cleaning step. These patches were distributed randomly and exhibited a residual thickness less than 5µm.

RESULTS AND DISCUSSION

Thermal resistance analysis

The thermal resistance was evaluated regularly over the 5 cycles of paraffin coating and online cleaning experiments. The R values for the first and fifth cycles are presented in Figure 7. Also shown is a data set from a control test, conducted without any paraffin coating, in which case $R = R_f$, the fouling resistance due to biofilm formation. The profiles show an initial lag phase in which there is little change in R followed by a period of steady growth. The control data set show an almost linear increase in R whereas those with the paraffin coating exhibit a sigmoidal trend, approaching an asymptote after 5 days.

The construction in Figure 7 shows how R is composed of two terms, R_f and R_{add} . The paraffin coating gives a sizeable R_{add} value, at $0.27 \times 10^{-4} \text{ m}^2 \text{ K} \cdot \text{W}^{-1}$ for the first cycle, while reducing R_f to $1.48 \times 10^{-4} \text{ m}^2 \text{ K} \cdot \text{W}^{-1}$ (a difference of by $0.50 \times 10^{-4} \text{ m}^2 \text{ K} \cdot \text{W}^{-1}$ compared to the control data set). The total R decreased by $0.23 \times 10^{-4} \text{ m}^2 \text{ K} \cdot \text{W}^{-1}$ compared to the control group.

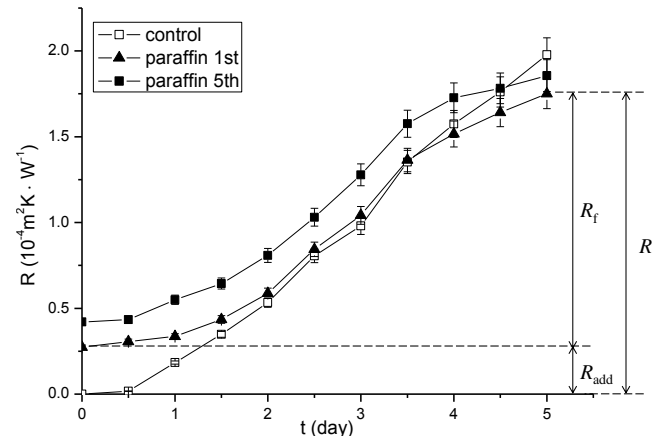


Fig. 7 Evolution of total thermal resistance, R , for first fouling cycle, fifth fouling cycle and control (no paraffin layer). Construction on right shows how the components of R are calculated (Equation (3)).

Figure 7 shows that biofouling was influenced significantly at two stages: the initial attachment stage and the asymptotic stage. The former is attributed to the hydrophobicity and change in roughness reducing the rate of initial attachment of bacteria cells. Another factor is that the additional thermal resistance, R_{add} , modifies the initial model fluid–paraffin interface temperature, giving a cooler surface than the model fluid–SS interface temperature in the control test, which may also contribute to the inhibition of biofouling at initial stage. The low roughness can also favour detachment of a biofouling layer from the paraffin layer, leading to the reduction in R_f during the asymptotic stage.

The primary purpose and advantage of the paraffin coating is the improvement of online cleaning, and it is accepted that the fouling inhibition effect may be relatively weak in comparison to other surface coating methods. The inhibition effect should be considered as sufficient if R_{add} is balanced by the reduction in R_f over the timescale of interest: this is considered further in the techno-economic analysis. The reduction in biofouling could be enhanced by the use of materials other than paraffin, or by incorporating biofouling inhibition agent(s) such as silver nanoparticles into the paraffin coating. Ideally these agents, like the coating, should be recoverable from the cleaning fluid and recycled.

The individual components of R are reported in Figure 8. Error bar stands for measurement error. The contribution from biofouling, R_f , is relatively constant over the five cycles.

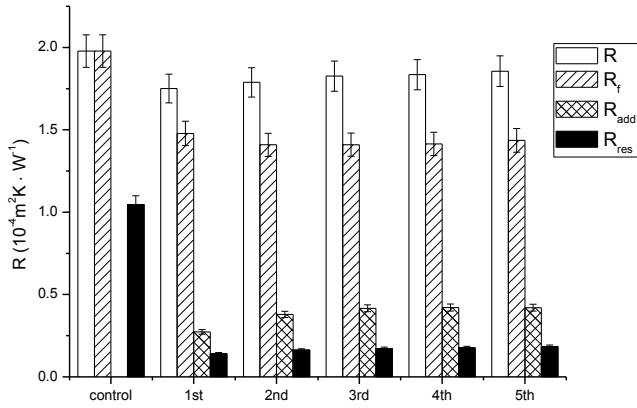


Fig. 8 Summary of overall thermal resistance, R , and components R_f , R_{add} and R_{res} at the end of each cycle and control group (R_{add} for the control group is 0, by definition). R_{res} was measured after online cleaning of each cycle.

Additional thermal resistance

The additional resistance due to coating, R_{add} , increases slightly over the first three cycles and is constant thereafter. R_{add} consists of two parts (Equation (2)): the additional resistance due to conduction across the wax layer, $R_{add,P}$, and the contact resistance, $R_{add,C}$, illustrated in Figure 9. The former can be estimated from the measured thermal conductivity, (λ ; $0.27 \text{ W m}^{-1}\text{K}^{-1}$) and thickness (δ ; $6.3\mu\text{m}$) of the paraffin coating, via $R_{add,P} = \delta/\lambda = 0.23 \times 10^{-4} \text{ m}^2\text{K} \cdot \text{W}^{-1}$. This represents 85% of R_{add} for the first cycle: $R_{add,C}$ is estimated by difference at $0.04 \times 10^{-4} \text{ m}^2\text{K} \cdot \text{W}^{-1}$. This is equivalent to conduction through a $2.4 \mu\text{m}$ thick water film.

The $R_{add,P}$ value could be reduced by better control of the coating process to give a thinner layer as well as the use of a material with a higher thermal conductivity material. The range of suitable materials with suitable properties, including being adherent to steel while rejecting biofilms, affordable and recyclable are limited. $R_{add,C}$ was relatively small yet could still be reduced by better control of the coating process and use of surfactants to improve film attachment and homogeneity of the wax layer.

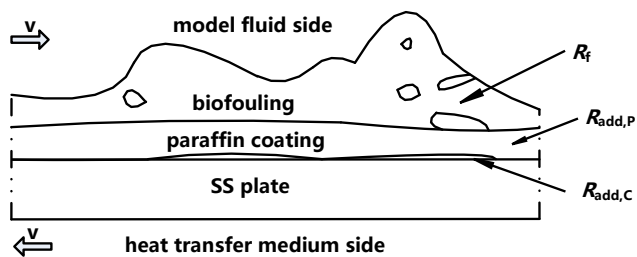


Fig. 9 Schematic of paraffin coating in fouling service showing origin of thermal resistances.

Residual thermal resistance

Figure 8 shows that the residual paraffin coating remaining after cleaning R_{res} increased slightly from the first cycle, from $0.14 \times 10^{-4} \text{ m}^2\text{K} \cdot \text{W}^{-1}$ to $0.18 \times 10^{-4} \text{ m}^2\text{K} \cdot \text{W}^{-1}$. By comparison, R_{add} approaches a value of $\sim 0.4 \times 10^{-4} \text{ m}^2\text{K} \cdot \text{W}^{-1}$,

so $R_{res} \approx 0.35R_{add}$. The observation of a steady R_{res} value is attributed to the use of similar cleaning processes. The similarity in R_{add} values across the cycles is attributed to the use of similar materials and, in particular, similar operating conditions.

Applying the same cleaning protocol to the uncoated plates gave $R_{res} = 1.05 \times 10^{-4} \text{ m}^2\text{K} \cdot \text{W}^{-1}$, which is nearly an order of magnitude larger than the coated surfaces. This illustrates the efficacy of the paraffin online cleaning concept. The difference is related to the microstructure of the biofilm, which Yang *et al.* (2013) reported as consisting of two layers: a softer, fluffy upper layer in contact with the solution and a dense and rigid layer adjacent to the substrate. Salley *et al.* (2012) showed that the mechanical strength of the two layers in a cyanobacteria biofilm can differ markedly. Hence, the main effect of the paraffin coating assistance is to promote the removal of the surface layer. The shear stress induced by the cleaning regime is sufficient to remove the fluffy layer, but growth can restart readily on the residual surface layer.

Techno-economic analysis

The experimental results above demonstrate that the paraffin coating method offers advantages over the existing practice in allowing fast on-line cleaning and inhibiting biofouling. However, the paraffin coating concept employs a coating-fouling-cleaning cycle, which requires additional equipment and periodic consumption of paraffin and excess thermal energy. The additional thermal resistance, R_{add} , from the coating will also affect the system’s capacity and efficiency compared to the existing protocol which employs regular, time-consuming, manual cleaning.

A techno-economic analysis was performed to establish the attractiveness for industrial application of the paraffin coating method. The industrial TSSHPS units are typically operated for 30 days between manual cleaning actions. The measured rate of fouling thermal resistance increase in those devices is about 6 times slower than those observed in these experiments, based on a comparison of the time duration for the thermal resistance to reach its asymptotic value (Zan et al., 2009). Manual cleaning takes 3 days to disassemble, clean and reassemble the TSSHPS plate heat exchanger. Given that biofilm ageing is more significant in the TSSHPS units due to their extended and slow fouling period, the time for cleaning and coating should also be extended. The online cleaning and re-coating processes takes about 2 hours to complete in the laboratory tests: the industrial units may need up to 12 hours for online cleaning and re-coating. Therefore, the TSSHPS operation period can be extended to 32.5 days using paraffin coating. Annualised costs were calculated for the two scenarios on the basis of 1 m^2 heat transfer area.

Figure 10 shows the estimated heat flux values over one cycle (33 days) of operation for each option. The induction period is 2 days for manual cleaning and 4 days for paraffin coating due to the initial inhibition by the coating layer. The coating concept units spend more time in service but they

give a lower initial heat flux than the mechanically cleaned units owing to the presence of the coating layer.

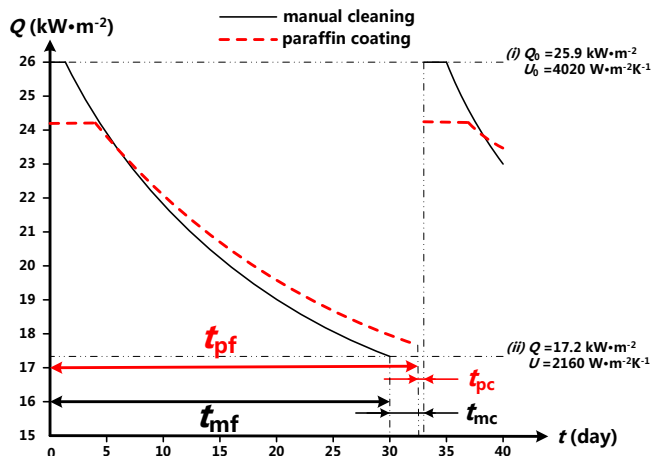


Fig. 10 Predicted effect of coating and fouling on heat flux in TSSHPS units. t_{mf} – fouling period for manual cleaning method, t_{pf} – fouling period for paraffin coating method, t_{mc} – period for manual cleaning, t_{pc} – cleaning period, paraffin coating. Horizontal dashed lines show (i) maximum value of Q (100% instantaneous profit) and (ii) lower, break even value (45% profit).

The typical daily running cost of a single TSSHPS system is €5 per day per m^2 plate heat exchanger surface for working period and €0.83 per day per m^2 for cleaning period.

The income was calculated based on the cooling duty delivered, at $0.50 \text{ € kW}^{-1}\text{day}^{-1}$. This indicates that there would be almost no profit if U decreased to $1150 \text{ W m}^{-2}\text{K}^{-1}$, corresponding to the heat flux falling to around 10 kW m^{-2} . Cleaning is usually started if the profit drops to 40~50% of the clean condition. This is taken as the break even value.

The average daily profit (before cleaning cost) was calculated from

$$P = \frac{\int_0^{t_f} I - \int_0^{t_f+t_c} C}{t_f + t_c} \quad (4)$$

where P , I and C are the average daily profit, the daily income and the daily running cost. t_f and t_c are the fouling period (working period) and cleaning period, respectively. Average daily profits (before cleaning cost) were 5.21 € m^{-2} for manual cleaning and 5.47 € m^{-2} for paraffin coating.

The similarity in average daily profit before cleaning indicates that cleaning costs are likely to be decisive. The estimated cost for a typical manual cleaning operation is 17.50 € m^{-2} for labour and cleaning supplies, and 1.25 € m^{-2} for abrasion costs. This gives a net daily profit for manual cleaning of 4.64 € m^{-2} .

The paraffin on-line cleaning and re-coating stages are costed in terms of paraffin consumption and energy use for cooling and heating. The plate gap is 5 mm and the liquid volume is 5 L m^{-2} heat transfer surface. A volume of wax

emulsion equivalent to ten times this volume is necessary for re-circulation, and its temperature needs to be raised from 20 °C to 70 °C for the coating and online cleaning steps. The total energy consumption is estimated as 31.5 MJ (10.5 MJ for emulsion heating during coating, 10.5 MJ for the process stream and 10.5 MJ for the heat transfer medium during cleaning). Using an electrical heater gives an energy cost of 0.53 € m^{-2} . This cost would be reduced if a suitable source of low-grade thermal energy was available.

Paraffin consumption and cost is an important factor: coating with 1 kg m^{-2} incurs 18.75 € m^{-2} and gives a net daily profit of 4.90 € m^{-2} if the emulsion is used only once. Reuse of the paraffin coating emulsion is therefore essential for financial as well as environmental benefits. The experimental data indicate that around 0.5 wt% of the paraffin in the emulsion is incorporated in the coating layer, and the emulsion can be, theoretically used continually as long as wax make-up is provided. The small amount of wax in the coating is therefore present as small concentrations in the cleaning solution and at this stage is not worthwhile to extract and reuse.

A conservative estimate is that the coating emulsion is used 10 times before replacement, *i.e.* annual replacement. The daily net profit, including cleaning costs, is then 5.39 € m^{-2} , which is 16% higher than the value for manual cleaning (4.64 € m^{-2}). Modifications to the coating process to give a thinner wax layer would increase profits further by reducing wax consumption and increasing heat transfer.

For a typical 12.5 MW capacity TSSHPS system with 500 m^2 heat exchanger surface, the annual benefit is estimated as $€ 67,6 \text{ k€ yr}^{-1}$, while the initial investment for a paraffin coating system is estimated as $€ 125,000$. The initial investment can be reduced to $€ 75,000$ if the paraffin coating system can share the heat transfer medium pump and piping with the TSSHPS, giving a payback time of approximately one year.

CONCLUSIONS AND PROSPECTS

1. Paraffin wax has been demonstrated to be an effective material for this new method of biofouling inhibition and online cleaning. It is readily available, affordable, and suitable for use with aqueous systems. It is biodegradable. These results also provide guidance for further research into alternative coating materials that may offer higher thermal conductivity and greater inhibitory effects.
2. The experimental results demonstrate that the concept is practicable: coating formation, biofouling inhibition and online cleaning cycles were all achieved. If a biofouling inhibiting agent could be incorporated into the paraffin coating, the inhibition effect would be enhanced and total thermal resistance reduced.
3. The residual paraffin coating was small (Biot number is 0.07) and the accumulation of residual material reached a steady state after 3-5 cycles.

4. A preliminary techno-economic analysis confirmed the feasibility of the concept and reinforced the need to reuse the coating solution.

ACKNOWLEDGMENTS

This work was supported by the National Natural Science Foundation of China (Grant No. 51236004), National Basic Research Program of China (Grant No. 2010CB227305) and a Tsinghua-Cambridge-Mong scholarship for Q. Yang.

NOMENCLATURE

Roman

Q	heat flux, $W\ m^{-2}$
Q_0	clean surface heat flux, $W\ m^{-2}$
R	thermal resistance, $m^2\ K\ W^{-1}$
R_a	surface roughness, m
R_{add}	additional thermal resistance, $m^2\ K\ W^{-1}$
$R_{add,P}$	additional conduct thermal resistance, $m^2\ K\ W^{-1}$
$R_{add,C}$	additional contact thermal resistance, $m^2\ K\ W^{-1}$
R_f	biofouling thermal resistance, $m^2\ K\ W^{-1}$
R_{res}	residual thermal resistance, $m^2\ K\ W^{-1}$
U	heat transfer coefficient, $W\ m^{-2}\ K^{-1}$
U_0	clean surface heat transfer coefficient, $W\ m^{-2}\ K^{-1}$

Greek

δ	thickness, m
λ	thermal conductivity, $W\ m^{-1}\ K^{-1}$

Subscript

add	additional
f	fouling
res	residual
0	clean surface

Acronyms

BOD	biological oxygen demand
CFU	colony forming unit
COP	coefficient of performance
PCR	polymerase chain reaction
SS	stainless steel
TSSHPS	treated sewage source heat pump system

REFERENCES

- Bonin, M.M., Duviau, M.P., Ellero, C., Lebleu, N., Raynaud, P., Despax, B., Schmitz, P., 2012, Dynamics of detachment of *Escherichia coli* from plasma-mediated coatings under shear flow, *Biofouling*, Vol. 28(9), pp. 881-894.
- Carl, C., Poole, A.J., Sexton, B.A., Glenn, F.L., Vucko, M.J., Williams, M.R., Whalan, S., Nys, R.D., 2012, Enhancing the settlement and attachment strength of pediveligers of *Mytilus galloprovincialis* by changing surface wettability and microtopography, *Biofouling*, Vol. 28(2), pp. 175-186.
- Christine, F., Marie, M.J., Pierre, U.J., Fontaine, B., Noelle, M., Brigitte, C., Annick, L.M., Thierry, B., 2000, Influence of physicochemical properties on the hygienic

status of stainless steel with various finishes, *Biofouling*, Vol. 15(4), pp. 261-274.

De Vos, W.M., De Keizer, A., Cohen Stuart, M.A., Kleijn, J.M., 2010, Thin polymer films as sacrificial layers for easier cleaning, *Colloids and Surfaces A*, Vol. 358, pp. 6-12.

Elangovan, T., George, R.P., Kuppusami, P., Mangalaraj, D., Bera, S., Mohandas, E., Kim, D.E., 2012, Development of a CrN/Cu nanocomposite coating on titanium-modified stainless steel for antibacterial activity against *Pseudomonas aeruginosa*, *Biofouling*, Vol. 28(8), pp. 779-787.

Georgiadis, M.C., Papageorgiou, L.G., 2000, Optimal energy and cleaning management in heat exchanger networks under fouling, *Trans IChemE*, Vol. 78(2), pp. 168-179.

Hwang, G., Kang, S., El Din, M.G., Liu, Y., 2012, Impact of an extracellular polymeric substance (EPS) precoating on the initial adhesion of *Burkholderia cepacia* and *Pseudomonas aeruginosa*, *Biofouling*, Vol. 28(6), pp. 525-538.

Jalalirad, M.R., Malayeri, M.R., Preimesser, R., 2012, Online cleaning of tubular heat exchangers in water service systems using projectiles, *Desalination and Water Treatment*, Vol. 1, pp. 1-6.

Li, X.M., Ji, Y., He, T., Wessling, M., 2008, A sacrificial-layer approach to prepare microfiltration membranes, *Journal of Membrane Science*, Vol. 320, pp. 1-7.

Müller-Steinhagen, H., Malayeri, M.R., Watkinson, A.P., 2005, Fouling of heat exchangers-New approaches to solve an old problem, *Heat Transfer Engineering*, Vol. 26(1), pp. 1-4.

Olsen, S.M., Pedersen, L.T., Hermann, M.H., Kiil, S., Johansen, K.D., 2009, Inorganic precursor peroxides for antifouling coatings, *J. Coat. Technol. Res*, Vol. 6(2), pp. 187-199.

Raulio, M., Jarn, M., Ahola, J., Peltonen, J., Rosenholm, J.B., Tervakangas, S., Kolehmainen, J., Ruokolainen, T., Narko, P., Salonen, M.S., 2008, Microbe repelling coated stainless steel analysed by field emission scanning electron microscopy and physicochemical methods, *J Ind Microbiol Biotechnol*, Vol. 35, pp. 751-760.

Salley, B., Gordon, P.W., McCormick, A.J., Fisher, A.C., Wilson, D.I., 2012, Characterising the structure of photosynthetic biofilms using fluid dynamic gauging, *Biofouling*, Vol. 28(2), pp. 159-173.

Scardino, A.J., Nys, R.D., 2010, Mini review: Biomimetic models and bioinspired surfaces for fouling control, *Biofouling*, Vol. 27(1), pp. 73-86.

Schmidt, D.P., Shaw, B.A., Sikora, E., Shaw, W.W., Laliberte, L.H., 2006, Corrosion protection assessment of sacrificial coating systems as a function of exposure time in a marine environment, *Progress in Organic Coatings*, Vol. 57(4), pp. 352-364.

Sen, Y., Bagci, U., Gulec, H.A., Mutlu, M., 2012, Modification of Food-Contacting Surfaces by Plasma Polymerization Technique: Reducing the Biofouling of

Microorganisms on Stainless Steel Surface, *Food Bioprocess Technol*, Vol. 5(1), pp. 166-175.

Shi, L., Zan, C., Yang, W., 2009, Composition and morphology of composite fouling by municipal secondary effluent on heat transfer surfaces, *Journal of Tsinghua University (Science and Technology)*, Vol. 49(2), pp. 236-239.

Sokolova, A., Cilz, N., Daniels, J., Stafslie, S.J., Brewer, L.H., Wendt, D.E., Bright, F.V., Detty, M.R., 2012, A comparison of the antifouling/foul-release characteristics of non-biocidal xerogel and commercial coatings toward micro- and macrofouling organisms, *Biofouling*, Vol. 28(5), pp. 511-523.

Tian, L., Chen, X., Yang, Q., Chen, J., Li, Q., Shi, L., 2012a, Effect of silica dioxide particles on the evolution of biofouling by *Bacillus subtilis* in plate heat exchangers relevant to a heat pump system used with treated sewage, *Chemical Engineering Journal*, Vol. 188, pp. 47-56.

Tian, L., Chen, X., Yang, Q., Chen, J., Shi, L., Li, Q., 2012b, Effect of calcium ions on the evolution of biofouling by *Bacillus subtilis* in plate heat exchangers simulating the heat pump system used with treated sewage in the 2008 Olympic Village, *Colloids and surfaces B, Biointerfaces*, Vol. 94, pp. 309-316.

Vladkova, T., 2008, Surface modification approach to control biofouling, Springer-Verlag, Berlin, Heidelberg, pp. 135-163.

Wang, Y., Pitet, L.M., Finlay, J.A., Brewer, L.H., Cone, G., Betts, D.E., Callow, M.E., Callow, J.A., Wendt, D.E., Hillmyer, M.A., De Simone, J.M., 2011, Investigation of the role of hydrophilic chain length in amphiphilic perfluoropolyether/poly (ethylene glycol) networks: towards high-performance antifouling coatings, *Biofouling*, Vol. 27(10), pp. 1139-1150.

Wilson, M., Harvey, W., 1989, Prevention of bacterial adhesion to denture acrylic, *Journal of Dentistry*, Vol. 17(4), pp. 166-170.

Yang, Q., Wilson, D.I., Chen, X., Shi, L., 2013, Experiment investigation of interactions between the temperature field and biofouling in treated sewage, *Biofouling*, Vol. 29(5), pp. 513-523.

Zan, C., Shi, L., Ou, H., 2009, Effects of temperature and velocity on fouling by municipal secondary effluent in plate heat exchangers, *Journal of Tsinghua University (Science and Technology)*, Vol. 49(2), pp. 240-243.